Model Reduction of Coherent LPV Models in Power Systems

Johnny Leung*, Michel Kinnaert*, Jean-Claude Maun[†] and Fortunato Villella[‡]

* Department of Control Engineering and System Analysis

[†] Department of Bio-, Electro- And Mechanical Systems

Université libre de Bruxelles (ULB), Brussels, Belgium

{johnny.leung, michel.kinnaert, jcmaun}@ulb.ac.be

[‡] Elia Grid International (EGI), Brussels, Belgium

fortunato.villella@eliagrid-int.com

Abstract—This paper extends the applicability of a balancing-based reduction method to power system models that are structured into a study area, a buffer area, and a linear parameter-varying (LPV) external area. The latter is represented by a network of linear time-invariant (LTI) and LPV models and forms the target of the reduction phase. Every LPV model is built to depict a region of the power system with a variable number of active generators. The various LTI and LPV models are simplified while accounting for the presence of their respective neighbors. The adequacy of the reduction process is verified on the IEEE 118-bus system model by comparing the dynamic behavior of the reduced model and the full nonlinear model for different sets of disconnected generators.

Index Terms—balanced truncation, clusters, LPV model, power system stability, structured model reduction

I. Introduction

Modern power systems have experienced an increase in the number of interconnection lines and renewable energy sources over the past years. As a result, large quantities of electricity can be delivered over long distances to many customers. Yet, at the same time, there is no denying that this transition brings new challenges in terms of planning, operation, and control. In particular, running dynamic simulations on an accurate power system model tends to be computationally very demanding for the purpose of short-term stability studies.

Previous research on model reduction has come up with some solutions to the described problem [1]–[4], but these fail at providing enough flexibility to incorporate later changes in the power system. The reduced models are only valid around the operating conditions they were derived from and cannot accommodate to a shift in energy production and consumption. This major restriction implies that the reduction algorithm needs to be relaunched after any noticeable change, which may negate the time saved during the simulations.

With a view of addressing this shortcoming, a parallel work was performed to represent a region within a power system by a linear parameter-varying (LPV) model [5]. The unique scheduling parameter is arranged to reflect a change in the number of active generators inside the related region. Another work focuses on the structured model reduction of coherent clusters in a power system [6]. The mathematical model of each cluster is linearized about an equilibrium point and reduced in a way that preserves the global behavior of the power system at best. In this paper, the objective is to extend the applicability of the same structured model reduction algorithm to a set of LPV models belonging to the external area of a power system. The expected outcome is a reduced model that can be tuned according to different loading conditions of the power system.

The rest of this paper is organized as follows. Section II introduces the problem to be solved and shows the general form given to the LPV models. Section III recalls the working principle of the structured model reduction algorithm and discusses the extension to LPV models. Section IV analyzes the performance of the reduction approach on the IEEE 118-bus system model in which the different regions of the external area have been replaced by LTI or LPV models.

II. Problem Statement

Consider a power system model that is composed of a nonlinear study area, a nonlinear buffer area, and a linear external area (see Fig. 1). The buffer and the external areas are furthermore partitioned into coherent clusters, i.e., several groups of busbars that are oscillating in phase upon occurrence of any disturbance initiated within the study area. The interactions between clusters and with the study area are governed by a series of tie-lines connected to some busbars [3], [6]. For a given cluster, the voltage magnitudes V^{out} and phase angles θ^{out} of the busbars located at the internal end of the tie-lines form the set of outputs $\boldsymbol{y}$. Instead, the voltage magnitudes V^{in} and phase angles θ^{in} of the busbars at the external end of the tie-lines represent the set of inputs $\boldsymbol{u}$ (see example in Fig. 1).

The general objective is to simplify the cluster models of the linear external area while restricting the impact of the simplification on the dynamic behavior of the study area. Unlike in [6], only some of the clusters are depicted by linear time-invariant (LTI) models, whereas the others are represented by LPV models of the following form

$$\begin{aligned} \Delta\dot{\boldsymbol{x}} &= \boldsymbol{A}(\alpha)\Delta\boldsymbol{x} + \boldsymbol{B}(\alpha)\Delta\boldsymbol{u} \\ \Delta\boldsymbol{y} &= \boldsymbol{C}(\alpha)\Delta\boldsymbol{x} + \boldsymbol{D}(\alpha)\Delta\boldsymbol{u} \end{aligned} \tag{1}$$
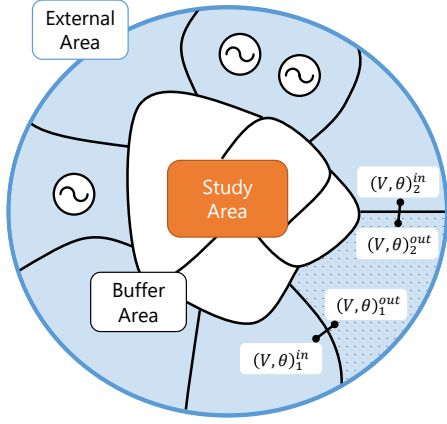
Fig. 1. Illustration of a network partitioning into a study area, a buffer area, and an external area. The clusters of the external area (in blue) are either turned into LTI or LPV models. The input and output signals depicted in the figure hold for the cluster with the dotted pattern.

where $\Delta \boldsymbol{x} \in \mathbb{R}^n$ is the vector of n state variables, $\Delta \boldsymbol{u} \in \mathbb{R}^m$ is the vector of m inputs, and $\Delta \boldsymbol{y} \in \mathbb{R}^p$ is the vector of p outputs. The matrices $\boldsymbol{A}(\alpha) \in \mathbb{R}^{n \times n}$, $\boldsymbol{B}(\alpha) \in \mathbb{R}^{n \times m}$, $\boldsymbol{C}(\alpha) \in \mathbb{R}^{p \times n}$, and $\boldsymbol{D}(\alpha) \in \mathbb{R}^{p \times m}$ characterize the LPV state-space representation of a cluster and present the following parametric dependence

$$\boldsymbol{A}(\alpha) = \boldsymbol{A}_0 + \sum_{j=1}^{n_p} (1-\alpha)^j \boldsymbol{A}_j \qquad \boldsymbol{C}(\alpha) = \boldsymbol{C}_0$$

$$\boldsymbol{B}(\alpha) = \boldsymbol{B}_0 + \sum_{j=1}^{n_p} (1-\alpha)^j \boldsymbol{B}_j \qquad \boldsymbol{D}(\alpha) = \boldsymbol{D}_0$$

(2)

The scheduling parameter α reflects a change in the number of active generators within a cluster and is tuned by computing the ratio of the total kinetic energy in the new situation to the total kinetic energy in the reference case [5]

$$\alpha = \frac{\sum_{G \in \mathbf{G}_{\text{new}}} H_G S_G}{\sum_{G \in \mathbf{G}_{\text{ref}}} H_G S_G}$$

(3)

where $\mathbf{G}_{\text{ref}}$ is the group of active generators in the reference case, $\mathbf{G}_{\text{new}}$ is the group of active generators in the new situation, H_G is the inertia constant, and S_G is the nominal apparent power of the Gth generator.

To simplify a LPV model (1) with an affine parametric dependence (2), an efficient strategy is to find a pair of basis matrices $\boldsymbol{V}$ and $\boldsymbol{W}$ such that [7], [8]

$$\hat{\boldsymbol{A}}(\alpha) = \boldsymbol{W}^T \boldsymbol{A}_0 \boldsymbol{V} + \sum_{j=1}^{n_p} (1-\alpha)^j \boldsymbol{W}^T \boldsymbol{A}_j \boldsymbol{V}$$

$$\hat{\boldsymbol{B}}(\alpha) = \boldsymbol{W}^T \boldsymbol{B}_0 + \sum_{j=1}^{n_p} (1-\alpha)^j \boldsymbol{W}^T \boldsymbol{B}_j$$

(4)

All the reduced-order matrices $\boldsymbol{W}^T \boldsymbol{A}_j \boldsymbol{V}$ and $\boldsymbol{W}^T \boldsymbol{B}_j$ can then be precomputed in the offline phase while the resulting

matrices $\hat{\boldsymbol{A}}(\alpha)$ and $\hat{\boldsymbol{B}}(\alpha)$ keep a parametric dependence. The general objective hence amounts to finding appropriate basis matrices $\boldsymbol{V}$ and $\boldsymbol{W}$ for every LTI and LPV models within the external area.

III. COHERENT CLUSTERING BALANCED TRUNCATION

A power system model whose buffer and external areas are partitioned into coherent clusters is compatible with the coherent clustering balanced truncation (CCBT) reduction method originally developed in [6] for LTI cluster models. In [6], this method replaces every coherent cluster of the external area by a reduced-order LTI equivalent while taking into consideration the presence of their respective neighbors.

Concretely, suppose that a relative level of proximity is assigned to the different clusters (see Fig. 2). Each cluster is recognized as the central cluster throughout its own reduction stage. The adjacent clusters sharing a connection with the central cluster form the first layer of clusters $L1$. In turn, the clusters connected to the cluster in $L1$ compose the second layer of clusters $L2$, and so on. The CCBT method simplifies a central cluster by building a custom linear equivalent system with the clusters in $L1$ and using it as frequency weight during the reduction phase.
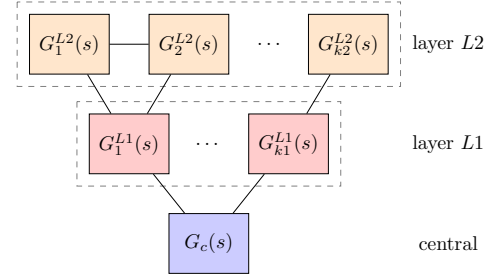

Fig. 2. Example of an arrangement of clusters into multiple layers. The clusters are either part of the external area or of the buffer area.

A. Constructing an Equivalent System for Each Cluster

Assuming that $k1$ clusters belong to the first layer $L1$ associated with a given cluster, a linear state-space realization of the small interconnected system, comprising the central cluster and the layer $L1$, is represented as [6]

$$\Delta \dot{\boldsymbol{x}}^e = \boldsymbol{A}^e \Delta \boldsymbol{x}^e + \boldsymbol{B}_\theta^e \Delta \boldsymbol{\theta}^e$$

$$\Delta \boldsymbol{y}^e = \boldsymbol{C}^e \Delta \boldsymbol{x}^e + \boldsymbol{D}_\theta^e \Delta \boldsymbol{\theta}^e$$

(5)

where $\Delta \boldsymbol{x}^e \in \mathbb{R}^{n^e}$ is the vector of n^e state variables, $\Delta \boldsymbol{y}^e \in \mathbb{R}^{p^e}$ is the vector of p^e outputs, $\Delta \boldsymbol{\theta}^e \in \mathbb{R}^{k2}$ is the vector of $k2$ inputs.

The vector of state variables $\Delta \boldsymbol{x}^e$ are arranged as

$$\Delta \boldsymbol{x}^e = \begin{bmatrix} (\Delta \boldsymbol{x}_c)^T & (\Delta \boldsymbol{x}_1^{L1})^T & \dots & (\Delta \boldsymbol{x}_{k1}^{L1})^T \end{bmatrix}^T$$

where $\Delta \boldsymbol{x}_c \in \mathbb{R}^{n_c}$ corresponds to the central cluster, $\Delta \boldsymbol{x}_j^{L1} \in \mathbb{R}^{n_j^{L1}}$ corresponds to the jth cluster inside the layer $L1$, and $n_c + \sum_{j=1}^{k1} n_j^{L1} = n^e$. The $n_{1 \leftrightarrow 2}$ tie-lines between the $k1$

clusters of the first layer $L1$ and the $k2$ clusters of the second layer $L2$ determine the vector of outputs $\Delta\boldsymbol{y}^e$ of the small interconnected system

$$\Delta\boldsymbol{y}^e = \left[(\Delta\boldsymbol{\theta}_{1\leftrightarrow2}^{out})^T \quad (\Delta\boldsymbol{V}_{1\leftrightarrow2}^{out})^T\right]^T$$

where $\Delta\boldsymbol{\theta}_{1\leftrightarrow2}^{out} \in \mathbb{R}^{n_{out}}$ and $\Delta\boldsymbol{V}_{1\leftrightarrow2}^{out} \in \mathbb{R}^{n_{out}}$ are associated with n_{out} busbars of the first layer $L1$. The vector of inputs $\Delta\boldsymbol{\theta}^e$ withholds one entry per cluster of the second layer $L2$

$$\Delta\boldsymbol{\theta}^e = \left[\Delta\theta_1^{in} \quad \Delta\theta_2^{in} \quad \ldots \quad \Delta\theta_{k2}^{in}\right]^T$$

where $\Delta\theta_j^{in} \in \mathbb{R}$ is a substitute for all the voltage phase angles belonging to the jth cluster of the second layer $L2$.

B. Reducing the Central Cluster

The interconnected system balanced truncation (ISBT) method [3], [6], [9], [10] is applied for extracting the relevant modes of the central cluster inside the larger system (5). In this context, the first step consists in computing the controllability $\boldsymbol{P}^e$ and observability $\boldsymbol{Q}^e$ Gramians, which are the solutions to the following Lyapunov equations

$$\begin{aligned} \boldsymbol{A}^e\boldsymbol{P}^e + \boldsymbol{P}^e(\boldsymbol{A}^e)^T + \boldsymbol{B}_\theta^e(\boldsymbol{B}_\theta^e)^T &= 0 \\ (\boldsymbol{A}^e)^T\boldsymbol{Q}^e + \boldsymbol{Q}^e\boldsymbol{A}^e + (\boldsymbol{C}^e)^T\boldsymbol{C}^e &= 0 \end{aligned} \quad (6)$$

Each row/column in $\boldsymbol{P}^e$ and $\boldsymbol{Q}^e$ is related to a state variable of $\Delta\boldsymbol{x}^e$, and the Gramians can be partitioned as

$$\boldsymbol{P}^e = \begin{bmatrix} \boldsymbol{P}_c & \cdots \\ \vdots & \ddots \end{bmatrix}, \quad \boldsymbol{Q}^e = \begin{bmatrix} \boldsymbol{Q}_c & \cdots \\ \vdots & \ddots \end{bmatrix} \quad (7)$$

where $\boldsymbol{P}_c$ and $\boldsymbol{Q}_c$ are $n_c \times n_c$ submatrices.

The balancing algorithm takes the upper left sub-Gramians $(\boldsymbol{P}_c, \boldsymbol{Q}_c)$ and finds a coordinate transformation $\Delta\boldsymbol{x}_c = \boldsymbol{S}\Delta\bar{\boldsymbol{x}}_c$ that makes the sub-Gramians balanced, namely $\bar{\boldsymbol{P}}_c = \boldsymbol{S}^{-1}\boldsymbol{P}_c\boldsymbol{S}^{-T}$ and $\bar{\boldsymbol{Q}}_c = \boldsymbol{S}^T\boldsymbol{Q}_c\boldsymbol{S}$ fulfill

$$\begin{aligned} \bar{\boldsymbol{P}}_c = \bar{\boldsymbol{Q}}_c &= \boldsymbol{\Sigma}_c = \text{diag}\left\{\sigma_1^c, \ldots, \sigma_n^c\right\} \\ \sigma_1^c &\geq \cdots \geq \sigma_n^c \\ \sigma_j^c &= \sqrt{\lambda_j(\boldsymbol{P}_c\boldsymbol{Q}_c)} = \sqrt{\lambda_j(\bar{\boldsymbol{P}}_c\bar{\boldsymbol{Q}}_c)}. \end{aligned} \quad (8)$$

where $\lambda_j(\boldsymbol{A})$ denotes the jth eigenvalue of the matrix $\boldsymbol{A}$. σ_j^c is a Hankel singular value of the studied cluster c and indicates how controllable and observable the jth variable of $\Delta\bar{\boldsymbol{x}}_c$ is with respect to the inputs $\Delta\boldsymbol{\theta}^e$ and the outputs $\Delta\boldsymbol{y}^e$ of the small interconnected system.

The order of the central cluster is reduced by discarding the state variables associated with low Hankel singular values.

C. Extending the CCBT Method to LPV Models

The LPV models are built around the expected operating conditions (OC) of the power system, which are retrieved by setting $\alpha = 1$. As can be seen from (3), this parameter value corresponds to the initial configuration where all the generators are maintained active. In this case, the cluster models (2)

amount to LTI state-space representations characterized by their respective matrices $\boldsymbol{A}_0$, $\boldsymbol{B}_0$, $\boldsymbol{C}_0$, $\boldsymbol{D}_0$.

To ensure a high quality for the reduced LPV models around the expected OC, the CCBT method is applied to the power system configuration where all scheduling parameters $\alpha = 1$. The main idea is to collect the truncated matrices $\boldsymbol{S}$ and $\boldsymbol{S}^{-T}$ and use them respectively as the requested basis matrices $\boldsymbol{V}$ and $\boldsymbol{W}$ for the reduction of the LPV models in (4). The reduced LPV models at $\alpha = 1$ would then coincide with the reduced LTI models at the expected OC as

$$\begin{aligned} \hat{\boldsymbol{A}}(1) &= \boldsymbol{W}^T\boldsymbol{A}_0\boldsymbol{V} & \hat{\boldsymbol{C}}(1) &= \boldsymbol{C}_0\boldsymbol{V} \\ \hat{\boldsymbol{B}}(1) &= \boldsymbol{W}^T\boldsymbol{B}_0 & \hat{\boldsymbol{D}}(1) &= \boldsymbol{D}_0 \end{aligned}$$

This reduction approach may not be as robust as when the basis matrices $\boldsymbol{V}$ and $\boldsymbol{W}$ are constructed after varying the vector of scheduling parameters $\boldsymbol{\alpha} = [\alpha_1 \ \alpha_2 \ \ldots \ \alpha_d]^T$ and sampling information within a domain $\Omega \subset \mathbb{R}^d$, where α_j is the scheduling parameter of the jth LPV model and d is the total number of LPV models inside the power system. Nevertheless, it is computationally less costly and becomes a viable solution when the subspaces spanned by the local basis matrices $\boldsymbol{V}\big|_\alpha$ and $\boldsymbol{W}\big|_\alpha$ do not deviate significantly from one realization of $\boldsymbol{\alpha}$ to another. This last point is verified in Section IV by showing that the angular deviation between corresponding basis matrices remains low in all circumstances.

IV. RESULTS

In this section, the performance of the CCBT reduction method is assessed on the IEEE 118-bus system model whose external area is replaced by a network of LTI and LPV models for the model reduction stage. The focus is on comparing the dynamic behavior of the study area in the reduced model to the one in the full nonlinear model. All the tests are conducted on PSAT, which is a Matlab toolbox for electric power system analysis and simulation.

A. IEEE 118-Bus System Model

Each generator, with $P > 0$, is represented by a 6th-order synchronous machine model, equipped with a IEEE type 1 excitation system and a type 1 turbine-governor. The generators, with $P \leq 0$, and the loads are all modeled as constant impedances.

Given an arbitrary study area, the rest of the power system has been divided into 8 coherent clusters. 2 of them (clusters 1 and 2) form the buffer area and the remaining ones (clusters 3 to 8) constitute the external area. Among the clusters of the external area, clusters 3, 4, 7, and 8 are represented by LPV models, whereas clusters 5 and 6 are just turned into LTI models, like in [5]. The degree n_p of the LPV models in the form of (2) are all set to 5. The outline of the different clusters are highlighted on Fig. 3.

B. Angles between Subspaces

A total of 2205 network configurations are considered to verify the possibility of reducing all clusters of the external area on the basis of only one network configuration. Each of
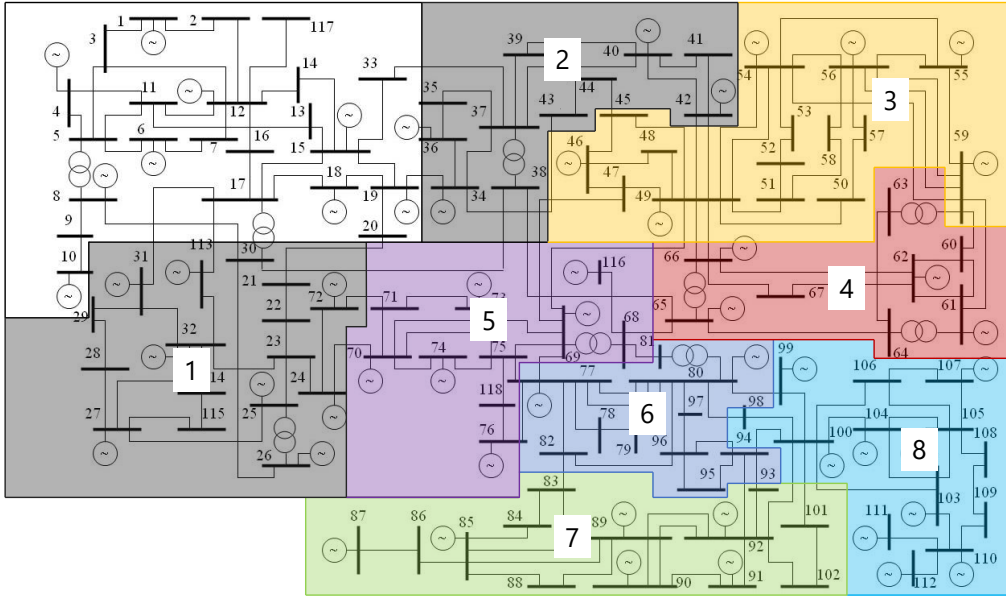
Fig. 3. IEEE 118-bus system. The blank cluster is the study area, the gray clusters form the buffer area, and the colored clusters constitute the external area.

them is obtained by tuning the α-value of the 4 LPV models and physically stems from a new situation with less active generators in the related clusters. From the definition in (3), the various α values are systematically confined within the range $]0,1]$ when excluding the situations leading to one or multiple clusters with no active generators.

Table I shows for every cluster the initial number of state variables n, the number of state variables $\hat{n}$ after reduction, the mean $\mu(\theta)$ and the maximum $\max(\theta)$ values of the largest principle angle θ [11], [12] between a local basis matrix $V|_\alpha$ and the reference one V_0. It can be observed that the angles between subspaces remain very small, irrespective of the network configuration under consideration. These numbers support the proposal of restricting the use of CCBT to a single realization of the vector $\boldsymbol{\alpha}$, namely $\alpha_j = 1, \forall j \in \{1,\ldots,d\}$.

TABLE I

Cluster #	n	$\hat{n}$	$\mu(\theta)$ (°)	$\max(\theta)$ (°)
3	52	10	2.22×10^{-6}	3.08×10^{-6}
4	39	9	2.06×10^{-6}	3.19×10^{-6}
5	13	5	1.62×10^{-6}	2.41×10^{-6}
6	13	5	1.68×10^{-6}	2.26×10^{-6}
7	26	4	1.79×10^{-6}	2.09×10^{-6}
8	39	7	2.06×10^{-6}	3.08×10^{-6}

C. Time Domain Simulation

After simplifying the clusters of the external area using CCBT, the quality of the resulting power system model is examined through time domain simulations. An electrical fault is applied inside the study area of both the reduced LPV model (*LPV*) and the full nonlinear model (*nonlinear*), and the focus is on comparing the time evolution of the same area.

To demonstrate the new flexibility offered by the *LPV* model, its scheduling parameters are tuned according to (3) to match two new situations with less active generators as shown in Table II, where the generators are recognized by the busbars they are connected to. The studied electrical fault is chosen to be a self-clearing short-circuit of 300 ms occurring at busbar 2, and the observed variable is the rotor speed of the generator connected to busbar 10.

TABLE II
CONFIGURATION OF THE CLUSTERS - SITUATIONS #1 AND #2

Cluster #	Initial GEN	#1	α_1	#2	α_2
3	46, 49, 54, 59	49	0.340	49	0.340
4	61, 65, 66	65	0.369	65	0.369
7	87, 89	89	0.979	89	0.979
8	100, 103, 111	100	0.499	100, 103, 111	1

In Fig. 4, it can be seen that the two models are overall in good agreement over the entire simulation period for both situations #1 and #2. With proper calibration, the *LPV* model is thus able to reproduce an adequate transient behavior, similar to the one obtained after disconnecting a set of generators.

Besides a series of time domain simulations, an eigenvalue analysis is also carried out on both types of model as a second confirmation test. 3 of the least damped oscillation modes are indicated in Table III. While the modes remain slightly different between the *LPV* and the *nonlinear* models, for the two considered situations, it can be noticed how mode 2 emerges simultaneously in both models under situation #2 only. The ability of the *LPV* model to capture comparable oscillation modes after calibration confirms its suitability for performing stability studies under different operating conditions.
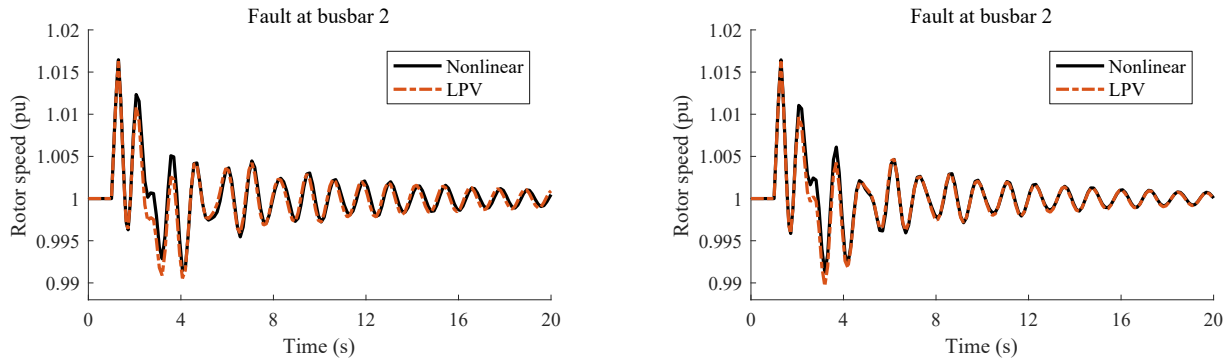
Fig. 4. Time evolution of a rotor speed signal belonging to the study area - Situation #1 (left) and Situation #2 (right).

TABLE III
EIGENVALUES OF THE LPV AND THE NONLINEAR MODELS[1]- SITUATIONS #1 AND #2

	Mode 1			Mode 2			Mode 3		
	λ_1	f_1 (Hz)	ζ_1 (%)	λ_2	f_2 (Hz)	ζ_2 (%)	λ_3	f_3 (Hz)	ζ_3 (%)
LPV #1	$-0.15 \pm j5.40$	0.86	2.76	-	-	-	$-0.26 \pm j8.41$	1.34	3.11
nonlinear #1	$-0.11 \pm j5.50$	0.87	2.00	-	-	-	$-0.27 \pm j8.06$	1.28	3.38
LPV #2	$-0.15 \pm j5.40$	0.86	2.76	$-0.63 \pm j6.30$	1.00	9.92	$-0.26 \pm j8.41$	1.34	3.11
nonlinear #2	$-0.13 \pm j5.27$	0.84	2.40	$-0.93 \pm j6.60$	1.05	13.92	$-0.28 \pm j8.06$	1.28	3.45

V. CONCLUSION

The possibility of applying the coherent clustering balanced truncation (CCBT) reduction method on an external area, which is composed of a network of linear time-invariant (LTI) and linear parameter-varying (LPV) models, is studied in this paper. The main concern is about the construction of the different basis matrices used for the projection-based reduction phase. In this context, a robust solution would require to sample information over the entire domain of variation of the scheduling parameters. However, the problem is that this strategy is computationally costly for large power system models. To limit the number of operations, the proposed alternative is to restrict the sampling procedure to one specific network configuration, namely the reference case around which the LPV models are built. The effectiveness of this strategy is successfully illustrated on the IEEE 118-bus system model by considering different sets of disconnected generators.

ACKNOWLEDGMENT

REFERENCES

[1] J. H. Chow, "Introduction," in *Power System Coherency and Model Reduction*, J. H. Chow, Ed. New York, NY: Springer New York, 2013, pp. 1–14.

[2] R. Podmore, "Coherency in power systems," in *Power System Coherency and Model Reduction*, J. H. Chow, Ed. New York, NY: Springer New York, 2013, pp. 15–38.

[3] C. Sturk, L. Vanfretti, Y. Chompoobutrgool, and H. Sandberg, "Coherency-independent structured model reduction of power systems," *IEEE Transactions on Power Systems*, vol. 29, no. 5, pp. 2418–2426, Sept 2014.

[4] S. D. Đukić and A. T. Sarić, "Dynamic model reduction: An overview of available techniques with application to power systems," *Serbian journal of electrical engineering*, vol. 9, no. 2, pp. 131–169, June 2012.

[5] J. Leung, M. Kinnaert, J.-C. Maun, and F. Villella, "Lpv modeling of clusters in dynamic power system models," in *2019 IEEE Milano PowerTech*, June 2019 (submitted), pp. 1–6.

[6] ——, "Model reduction of coherent clusters in power systems," in *2018 Mediterranean Conference on Power Generation, Transmission, Distribution and Energy Conversion (MedPower)*, Nov 2018, pp. 1–6.

[7] P. Benner, S. Gugercin, and K. Willcox, "A survey of projection-based model reduction methods for parametric dynamical systems," *SIAM Review*, vol. 57, no. 4, pp. 483–531, Nov 2015.

[8] U. Baur, C. Beattie, P. Benner, and S. Gugercin, "Interpolatory projection methods for parameterized model reduction," *SIAM Journal on Scientific Computing*, vol. 33, no. 5, pp. 2489–2518, Oct 2011.

[9] A. Vandendorpe and P. Van Dooren, "Model reduction of interconnected systems," in *Model Order Reduction: Theory, Research Aspects and Applications*, W. H. A. Schilders, H. A. van der Vorst, and J. Rommes, Eds. Berlin, Heidelberg: Springer Berlin Heidelberg, 2008, pp. 305–321.

[10] H. Sandberg and R. M. Murray, "Model reduction of interconnected linear systems," *Optimal Control Applications and Methods*, vol. 30, no. 3, pp. 225–245, May 2009.

[11] G. H. Golub and C. F. Van Loan, "Special topics," in *Matrix Computations (3rd Ed.)*. Baltimore, MD: The Johns Hopkins University Press, 1996, pp. 579–635.

[12] Å. Björck and G. H. Golub, "Numerical methods for computing angles between linear subspaces," *Mathematics of Computation*, vol. 27, no. 123, pp. 579–594, July 1973.

[1]For the eigenvalue analysis, the *LPV* and the *nonlinear* models are configured according to situations #1 and #2 and linearized about their respective equilibrium point.